

# The Hubble Space Telescope

## USEFUL IN SPITE OF THE MIRROR

G. Meylan

Space Telescope Science Institute  
Baltimore, Maryland, USA

Assessments of the Hubble Space Telescope (HST) and comparisons with ground-based observations of several well-studied astronomical objects demonstrate the instrument's unique observational capabilities. This is in spite of a by now commonly recognised flaw. Soon after launch in 1990, in-orbit testing of the HST revealed a serious optical problem with the 2.4 metre primary mirror. Prompted during the first two months of use by the consistent failure to align and focus the two (primary and secondary) mirrors of the telescope, a series of images was taken with the secondary mirror stepped through the full range of positions on each side of the nominal focus. These data showed conclusively that the anticipated sharp focus could not be obtained at any position of the secondary mirror. Moreover, images did not show the symmetric behaviour with respect to negative and positive offsets around the expected best focus position. It was concluded that the telescope suffers from a substantial amount of spherical aberration owing to an error introduced when the primary mirror was ground more than a decade ago.

A high angular resolution and the possibility to observe in the ultraviolet remain the telescope's main advantages. Its inherent problem and important potential will be illustrated using a few observations made with the Faint Object Camera (FOC), one of the European Space Agency's (ESA) contributions to the HST project.

### Less Photons — But Still Hawk-Eyed

The spherical aberration discovered in the HST optics gives rise to grossly defocused images in the telescope's focal plane at all settings of the secondary mirror. However, because one annulus of the primary mirror is always in focus at all settings between the foci of the outer and inner edges of the primary mirror (marginal and paraxial foci), the telescope point

Georges Meylan has been a Staff Astronomer with the Space Telescope Science Institute, 3700 San Martin Drive, Baltimore, MD 21218, USA, since 1989. He studied mathematics at the University of Lausanne, Switzerland, and astrophysics at the University of Geneva, receiving a Ph.D in 1985. He then held postdoc positions at the University of California, Berkeley, and at the Max-Planck-Institut, Garching, Germany.

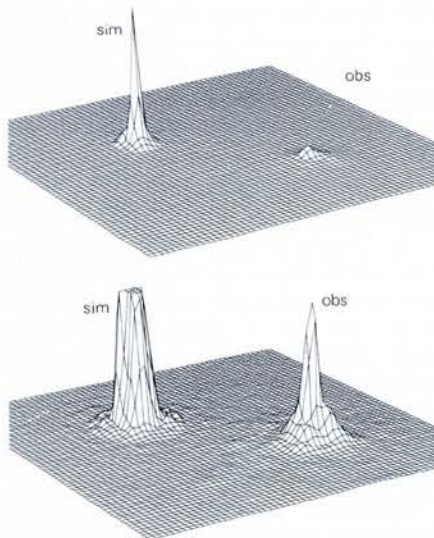
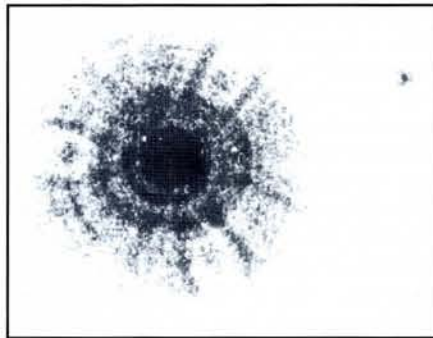


Fig. 1 — Image (in negative) of two stars located 10 arcmin East of  $\epsilon$  Scorpii obtained with the Faint Object Camera in the  $f/96$  mode through a filter with  $\Delta\lambda = 34 \text{ \AA}$  centred on  $\lambda = 4870 \text{ \AA}$ : the brighter star has a visible magnitude  $V = 12.3$ ; the second star is about 4.5 magnitudes fainter. The separation between the two stars is 6.3 arcsec. The bright star shows the central core surrounded by a large halo; the faint star has no halo, only its core emerges out of the background noise.

b, middle). The simulated, originally expected, point spread function (left) with the corresponding observed point spread function (right) obtained in orbit through the same filter. The actual core contains about 15% of the energy instead of the 80% expected, corresponding to a loss in sensitivity of about three orders of magnitude. c, lower) The same data as b) but with a different vertical scale: the sharp core is still present in the observed image so for bright objects, the resolving power of the telescope is retained.

spread function, *i.e.*, the image intensity distribution of a point source, possesses a sharp central core over a large range of secondary mirror positions.

ESA's Faint Object Camera consists of two independent optical relays, with effective focal ratios (focal numbers) of  $f/48$  and  $f/96$ , each of them being equipped with a photon counting detector capable of producing images using a variety of filters and prisms. Fig. 1 shows a FOC image of two stars located 10 arcmin East of  $\epsilon$  Scorpii obtained in the  $f/96$  mode through a filter with a wavelength range  $\Delta\lambda = 34 \text{ \AA}$  centred on a wavelength  $\lambda = 4870 \text{ \AA}$ . The fainter star has an intensity  $V$  in the visible wavelengths centred on approximately  $5500 \text{ \AA}$  which is a factor of about 4.5 times smaller than  $V$  for the brighter star: the separation between the two stars is 6.3 arcsec.

Although the exact focus position to be used may still change, the image can be regarded as representative of the present point spread function with its characteristic features, namely a sharp central bright core (Fig. 1, star on the left) and an extended faint halo (Fig. 1, star on the right). Several diffraction rings can be identified in the outer parts of the image of the bright star on the right: the larger outer ring structure is due to the shadow of the secondary mirror and the radial "tendrils" reflect the diffraction pattern of the secondary mirror support spider and mounting "pads" located on the primary mirror.

While the light from the star is spread over a circle with a diameter of almost 5 arcsec, the central peak of the image is nonetheless extremely sharp, even though it contains only 15% of the energy instead of the expected 80%. The loss of energy is clearly visible in Fig. 1b where the simulated, originally expected, point spread function (left) calculated for a point source with allowance for instrumental effects is presented, together with the observed function (right) obtained in orbit through the same filter for the bright star on the left of Fig. 1a. The intensity reduction is dramatic, corresponding to about three orders of magnitude. However, Fig. 1c demonstrates that, apart from some energy, everything has not been lost. The same simulated (left) and observed (right) point spread functions are displayed, but with a different vertical scale. A sharp

central core is still clearly present in the observed data and its diameter is only three pixels wide, corresponding to 0.066 arcsec at the full width half maximum (FWHM) intensity.

Thus, owing to the flaw in the primary mirror, the point spread function of the FOC has a tight diffraction-limited core, as expected originally, surrounded by an extended halo due to the spherical aberration. It is not so much the high spatial resolution of the HST cameras that has been compromised by the error in the mirror, but the limiting sensitivity.

It is worth emphasising that the astrophysical observations described below were made essentially to assess the HST's present capabilities. Consequently, they were done only for objects allowing comparison, *i.e.*, with those already been extensively observed with the most advanced ground-based techniques.

### An Ideal Case of Gravitational Lensing: The Einstein Cross

Since the first theoretical discussions more than 70 years ago on the phenomenon of light rays bent by intervening mass in the Universe — Eddington in 1920 for the case of the Sun, Einstein in 1936 for stars, and Zwicky in 1937 for galaxies — gravitational lensing has steadily grown to become one of the most active fields of research in extragalactic astronomy. There have been numerous theoretical investigations, but the number of candidates for which a body of evidence supports true lensing effects remains small. For it is only during the last decade that a few quasar systems have been found to be in reasonable agreement with the gravitational lensing interpretation.

Two astrophysical parameters relating to the lensed object, namely, high luminosity to reflect possible gravitational magnification and a large redshift to provide a large intercept length, increase the *a priori* probability that the object is lensed. Luminous quasars with large redshifts are ideal candidates. In case of perfect alignment and axial symmetry between 1) the lensed quasar in the background, 2) the lensing object in the foreground (generally the nucleus of a galaxy), and 3) the observer, the image of the quasar should form a ring centred on the nucleus of the galaxy. When ideal symmetry is lacking, the ring splits into several point images.

One of the best examples of gravitational lensing, G2237+0305, serendipitously discovered in 1985, involves a quasar at redshift  $z = 1.695$  and a less distant galaxy at redshift  $z = 0.039$ . This object is also called the Einstein Cross because of the characteristic four images of the quasar surrounding the nucleus of the galaxy. Already carefully studied and even monitored from the ground, the Einstein Cross was observed with the Faint Object Camera in order to explore the ability to

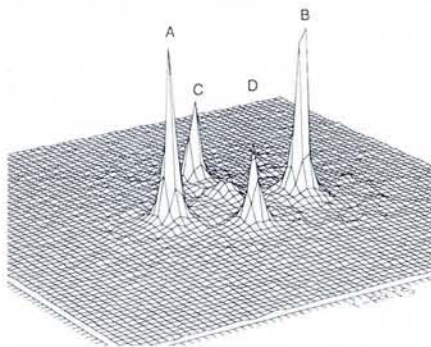


Fig. 2 — The Einstein Cross, or G2237+0305, taken by the Hubble Space Telescope with ESA's Faint Object Camera in the  $f/96$  mode through a filter centred on a wavelength  $\lambda = 4850 \text{ \AA}$  with an exposure time of 25 minutes: a, upper) The raw image showing that the single image of the quasar is split into (in this particular case) four images surrounding the nucleus of the galaxy. The nucleus of the intervening galaxy lies at only about 0.75 arcsec from the quasar images.

b, lower) Three-dimensional display. The bright cores of the four images (labelled A, B, C, and D) of the lensed quasar emerge out of the very bright background originating from the lensing galaxy, of which the nucleus is visible in the middle of the cross with a soft profile. The nucleus of the intervening galaxy is at only about 0.75 arcsec from the quasar images.

image closely spaced point sources in the presence of a background of galaxies.

A 25 minute exposure centred on  $\lambda = 4850 \text{ \AA}$  obtained in the FOC's  $f/96$  mode is reproduced in Fig. 2a: the same raw image is also displayed graphically in three dimensions in Fig. 2b. The bright cores of the four images (labelled A, B, C, and D) of the lensed quasar are well resolved, emerging out of the very bright background produced by both the lensing galaxy and the spherical aberration in the primary mirror. The resolution exceeds all previous ground-based image qualities (the FWHM of the FOC image is about 0.08 arcsec): the nucleus of the intervening galaxy, characterised by its soft profile, visible in the middle of the cross, is only about 0.75 arcsec from the images of the quasar.

### Microlensing

The photograph is ideal for accurately measuring the positions and brightness of the four quasar images — brightnesses which are already known to vary because of microlensing, when not only the whole potential of the galaxy is involved but also individual stars in their motions near the line of sight to the lensed quasar. This happens only when the lensing galaxy is relatively close to the observer. The (angular) proper motions of the stars are then fast enough to produce variations of the intensity of the images, hopefully on human time scales, *i.e.*, over some weeks, months or a few years at the most. Such conditions are met here owing to the unusually close proximity of the lensing galaxy, and variations in the relative intensities of the four images are observed.

We have found that the relative intensities have varied randomly over the last two years, *e.g.*, as shown in Fig. 2, the A component, formerly the brightest, is now fainter than component B — an effect caused by stars in the galaxy passing across the line-of-sight.

Thus, owing to the unusual position of the lensing galaxy, the large number of images produced, the relatively small time delay between images, and the likelihood of frequent microlensing events, the G2237 system represents an excellent candidate for monitoring lensing behaviour and for determining independent estimates of fundamental astrophysical parameters such as the Hubble constant  $H_0$ , a cosmological parameter linked to the age of the Universe.

### No Massive Star at the Core of the 30 Doradus Cluster

The Large Magellanic Cloud, a small neighbouring galaxy at a distance of about 55 000 pc (170 000 light years) contains the Tarantula Nebula — a huge, luminous complex made up of emitted gas and very young bright stars reminiscent of a large, hairy spider. Also called 30 Doradus, it contains in the central part a star cluster (NGC 2070) formed by a few hundreds of the most massive and brightest stars observed. The extreme core of this cluster, called R136a, is so luminous and so dense that it remained unresolved for a long time, so much so that it was thought in the early 1980's to contain a supermassive star — a single star with a mass of about 2000-3000 solar masses (more than ten times what is commonly thought to be the upper limit).

Although R136a was believed to consist of many young massive stars, previous ground-based images failed to resolve the hypothetical individual stars. Only by using some sophisticated ground-based observational techniques was it possible to show that no monster sat in this tangled core — one which clearly remained an ideal target for the HST.

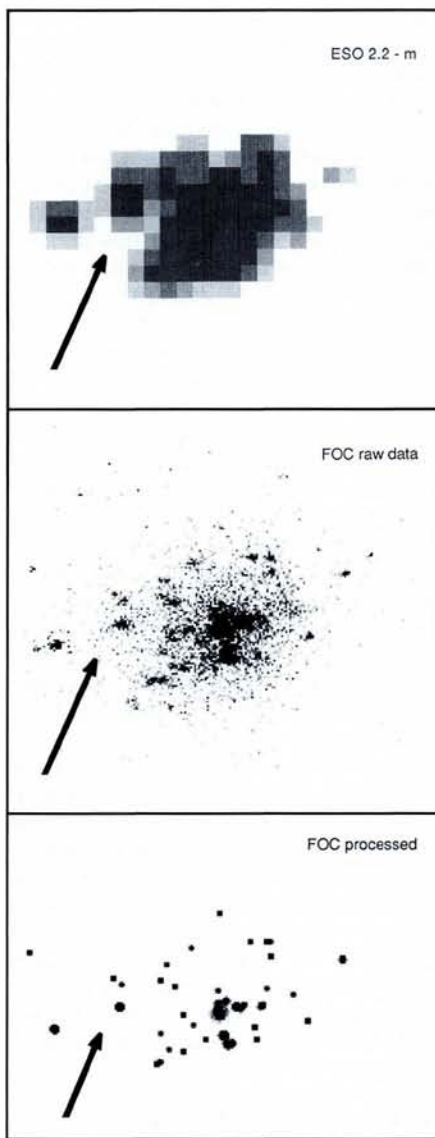


Fig. 3 — Three different views (in negative) of R136a, the core of 30 Doradus star cluster: a, upper) One of the best ground-based images, in this case taken with the 2.2 m telescope at the European Southern Observatory, La Silla, Chile, under excellent observing conditions (0.56 arcsec FWHM). b, middle) A raw Faint Object Camera image (at  $\lambda = 3460 \text{ \AA}$  in the f/96 mode) of the cluster core. c, lower) Processed version of b). The arrows in each figure indicate the same group of three stars which are clearly resolved in the raw FOC data, illustrating the telescope's high resolution by separating images of stars far more clearly than even the best conventional ground-based techniques. The field of view is  $10 \times 10 \text{ arcsec}^2$ .

The European Southern Observatory's 2.2 m telescope has provided us with Fig. 3a which is among the best ground-based images of R136a (taken under excellent observing conditions — 0.56 arcsec FWHM — without using any sophisticated techniques). A raw FOC image of the cluster core (at  $\lambda = 3460 \text{ \AA}$  in the f/96 mode) is shown in Fig. 3b. It illustrates the

high resolution of the HST and the ability to separate the stars far more clearly than even the best conventional ground-based photographs. For example, the three stars indicated in the figures by an arrow are clearly separated, even in the raw data, but are totally unresolved in the ground-based image.

The "haze" seen around the stars results from the effects of the spherical aberration of the primary mirror, which causes part of the light from the stars to be defocused. Nevertheless, for star clusters and similar kinds of relatively simple objects, computer processing techniques hold great promise for removing this haze. Fig. 3c shows the results of applying a deconvolution technique to the raw image using the known point spread function for the appropriate wavelength. The quality of the image has been improved ("restored") and what is already evident in the raw data is emphasised: there is no single supermassive star but instead an extremely rich and dense cluster of very young stars (they are roughly 100 times closer to each other than the Sun and its nearest neighbour). Moreover, each has a mass of about one hundred times the solar mass which, according to modern theories of star formation, is believed to be near the maximum possible mass.

An understanding of the detailed content of young clusters like R136a is important since it gives an observational upper limit to the mass of individual stars. Massive stars play an essential rôle in the formation of future generations of stars in their neighbourhood because of the important effect their intense energy output has on the surrounding interstellar gas. They also affect the evolution of galaxies through the synthesis of chemical elements, created via nuclear reactions deep in the star's interior, which are injected back into interstellar space by way of the supernova explosion occurring at the end of the star's life. Supernova 1987A is the most notable recent example, and this explosion took place in the 30 Doradus.

#### The Ashes of Supernova SN1987

Since the initial explosion of supernova SN1987 in February 1987, astronomers world wide have been closely monitoring its evolution using both ground-based and space instrumentation. SN1987 increased in brightness by a factor of 100 during the first three and a half years following the first observations, and then dimmed by one million times in brightness from the peak intensity. This dimming has enabled astronomers to take a closer look at the supernova proper and its surroundings.

Based on theoretical and spectroscopic evidence, SN1987A is known to be expanding rapidly, with the outer regions of the exploding star being ejected at an average speed of about 6000 kilometres per second. Hence, in the time span of three and

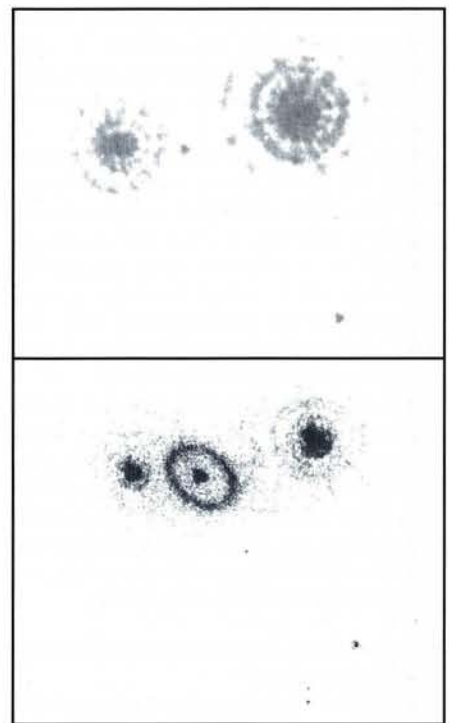


Fig. 4 — The supernova SN1987A (in negative): a, upper) A raw FOC image at  $\lambda = 1730 \text{ \AA}$  in the f/96 mode of SN1987A and its two bright companion stars. b, lower) The raw FOC image at  $\lambda = 5010 \text{ \AA}$  in the f/96 mode of the same field obtained through a narrow filter centred on a wavelength corresponding to the wavelength of the [O III] oxygen doublet emission line at  $\lambda = 4959$  and  $5007 \text{ \AA}$ : a beautiful circumstellar ring with a major axis of about 0.8 arcsec in diameter is revealed.

a half years the supernova should have grown to a diameter equivalent to approximately 0.1 light years, i.e., some 100 times larger than the solar system. As SN1987A is located 170000 light years away, its current angular size as seen from Earth would be expected to be about 0.1-0.2 arcsec in diameter. This angular extent is too small to be resolved with ground-based telescopes.

Comparisons between an image taken in ultraviolet light at  $\lambda = 2570 \text{ \AA}$  in the f/96 mode with the corresponding image of an unresolved reference star from the same exposure indicate that the SN1987A image is significantly broader than anticipated and extended in size. Although even the resolution of the FOC is still too coarse to clearly reveal much detailed structure, this is the first time that the exploding outer envelope of SN1987A has been photographed directly — a fact that clearly demonstrates the power of the HST, the spherical aberration of the telescope notwithstanding. The angular diameter of SN1987A measured from the images is  $\sim 0.15 \text{ arcsec}$ , i.e., close to expectations.

Other images (Fig. 4) of SN1987A and its surroundings taken with the FOC (at

$\lambda = 1730$  and  $5010 \text{ \AA}$  in the  $f/96$  mode) are shown in Fig. 4. The central object (Fig. 4a) is SN1987A itself and the bright objects on either side are relatively bright companion stars. The faint structures or halos surrounding these brighter stars are not real but result from the spherical aberration. The second image (Fig. 4b), taken using the light of twice ionised oxygen thanks to a narrow filter centred on a wavelength corresponding to the wavelength of the [O III] oxygen emission line doublet at  $4959$  and  $5007 \text{ \AA}$ , unveils a beautiful circumstellar luminescent structure surrounding SN1987A. This structure is most probably a ring and not a shell as the quantity of light emitted is low and the model agrees with other observations.

The existence of the ring had been gleaned previously from both ground-based and space observations in the ultraviolet. However, the FOC images have provided a much clearer view of its structure. The angular separation between the ring and SN1987A is estimated to be about  $0.8$  arcsec from the major axis — corresponding to  $0.75$  light years at the distance of the Large Magellanic Cloud. Being too large to have originated from material ejected by the supernova explosion, astronomers speculate that the ring (circular but seen at an angle of about  $\approx 1.5^\circ$ ) must have existed prior to the explosion as a ring of gas ejected and shaped by the "stellar winds" from the progenitor supergiant star some  $10\,000$  years prior to the supernova explosion. The ring material was then ionised and heated by the intense flash of ionising radiation emanating from the supernova. This radiation reached the ring within the year following the explosion and it is still glowing today, many years later. The presence of the ring thus provides astronomers with an important clue as to the nature and history of the progenitor star that exploded as the SN1987A supernova.

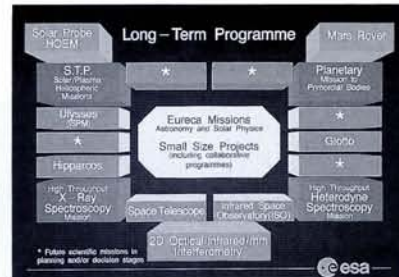
#### Future Developments

It is clear that the Hubble Space Telescope is not as powerful as it should have been because of a flaw. Nevertheless, the telescope is still extremely useful. Observations considered impossible from the ground are now acquired routinely.

Numerous studies have been made of a variety of possible remedies to the hardware problem. The most reasonable means for restoring the performance of the Faint Object Camera — and indeed those of the two other instruments — is widely recognised to consist in building and installing a device called COSTAR (Corrective Optics Space Telescope Axial Replacement) which would deploy corrective optics in front of each instrument's aperture. COSTAR is now fully funded and is scheduled to be mounted during the first maintenance mission with the Space Shuttle in early 1994.

## ESA's Scientific Programme

Dr. R.M. Bonnet, Director of the Scientific Programme of the European Space Agency (ESA), outlines the Agency's activities in the disciplines covered by the Programme, namely: exploration of the solar system, astronomy and fundamental physics.



ESA's Horizon 2000 long-term scientific programme for solar physics, astronomy and fundamental physics: major Cornerstone missions (boxed) having predefined objectives are augmented by competitive, Medium-Size Missions offering flexibility, and existing missions. There are also small projects as well as missions launched on the European Retrievable Carrier (EURECA).

#### Missions

The current missions are:

- the cometary probe *Giotto*, which, having flown by the nucleus of Comet Halley in 1985 has been redirected on to a trajectory leading to an encounter with Comet Grigg-Skjellerup in mid-1992;
- the *International Ultraviolet Explorer* (IUE), launched in 1978 and operated jointly with the US National Aeronautics and Space Administration (NASA) and the UK Science and Engineering Research Council since 1978 as an observatory facility;
- the astronomy satellite *Hipparcos*, launched in 1989, which will determine the positions, proper motions and parallaxes of  $120\,000$  stars with an accuracy of  $0.002$  arcsec;
- the *Hubble Space Telescope*, launched in 1990, a joint project with NASA in which ESA has a 15% share (see page 206);
- *Ulysses*, launched in 1990, a probe to explore the heliosphere at high latitudes, including the space over the poles of the Sun. This mission is also an ESA/NASA collaboration (see page 203).

The next mission to be launched will be the *Infrared Space Observatory* (ISO). This cryogenically cooled 60-cm telescope will be operated as an observatory facility starting in 1993. It covers the spectral domain from a few  $\mu\text{m}$  to  $200 \mu\text{m}$  and represents the only telescope of its class to fly in space until the early part of the next century.

#### Horizon 2000 Long-Term Plan

The centerpiece of ESA's long-term Horizon 2000 science programme, embarked upon in 1985, is a set of four *Cornerstone* missions, *i.e.*, major missions with scientific aims which were determined at the outset of the programme and which cover the interests of a broad segment of the European space research community as follows:

- solar system disciplines: *Solar-Terrestrial Science Programme* (the first Cornerstone — see page 213) and the return of a sample from a comet nucleus or an asteroid (*Rosetta*);
- astronomy: high-throughput X-ray (*XMM*) and sub-mm astronomy (*FIRST*).

The Cornerstones are augmented by a number of *Medium-Size Missions*, each selected competitively and — after four years of studies and evaluation — leads to the selection of a new project. The first Medium-Size Mission is *Huygens*, a probe to be launched in 1995 on NASA's Cassini spacecraft and to be released upon arrival at Saturn for a descent through the atmosphere of the moon Titan.

Four candidate projects for the *Second Medium-Size Mission* (M2) are presently being studied, prior to final selection in early 1993 and launch around about the year 2000. Two are astronomy missions, namely: an International Gamma-Ray Laboratory (INTEGRAL) and a mission to examine the asteroseismology and microvariability of stars (PRIMA); one is a solar system mission involving a set of meteorological and seismographic stations on Mars (MARSNET); the fourth is a Satellite Test of the Equivalence Principle (STEP) — a fundamental physics mission (see page 216).

#### ACKNOWLEDGEMENTS

The Faint Object Camera was built by the European Space Agency under the supervision of the Investigation Definition Team (IDT) with D.F. Macchetto as the Principal Investigator.

#### FURTHER READING

See *Astrophysical J. Lett.* **369** No. 2 Pt. 2 (1991) L21-L75 and **377** No. 1 Pt. 2 (1991) L1-L29 for detailed results and for interpretations of the scientific observations discussed in this article.